Large cell triaxial tests of a partially saturated soil with vegetation

Alessandro Fraccica[1*], *Enrique* Romero[2,3], and *Thierry* Fourcaud[4,5]

[1]Italian Institute for Environmental Protection and Research, ISPRA, Rome, Italy
[2]Geomechanics Group, CIMNE, Barcelona, Spain
[3]Department of Civil and Environmental Engineering, Universitat Politècnica de Catalunya, Barcelona, Spain
[4]CIRAD, UMR AMAP, F-34398 Montpellier, France
[5]AMAP, Université de Montpellier, CIRAD, CNRS, INRAE, IRD, Montpellier, France

Abstract. The use of vegetation roots as a nature-based solution against landslides and erosion requires the definition of sample preparation protocols and adoption of equipment that allows testing representative elementary volumes of the whole soil-root system. For this purpose, large cell triaxial compression tests were carried out on fallow and vegetated samples at different degrees of saturation. Samples were prepared by static compaction of a silty sand and seeded with *Cynodon dactylon*. The hydraulic state during plants growth was controlled and reproduced on bare soil samples. After isotropic compressions, the shearing phase was carried out at very low confining stresses (i.e., below 50 kPa). Tests were deemed to be comparable by assessing the normalised volume of roots with respect to soil, after shearing. For a given confining stress, soil samples with higher matric suction exhibited higher shear strength, furtherly increased by roots. The stress-strain behaviour observed in the vegetated soil systematically changed, when comparing tests at low and high matric suction values, due to the different mechanisms of vegetation reinforcement depending on the hydraulic state at the soil-root interface. The results were successfully interpreted within a failure criterion and skeleton stress framework for partially saturated soils, considering soil suction, degree of saturation, soil microstructure and the normalised volume of roots.

1 Introduction and background

Nature-based solutions, like the use of vegetation as reinforcement technique in slope stability or soil erosion problems are being commonly used by practitioners in natural areas and find increasing interest, given the actions against climate change and in favour of sustainable development. A fundamental step prior to important applications and the potential standardisation of such techniques is the quantification of the reinforcement and its correlation to given plant morpho-mechanical traits. In the literature, plant reinforcement on soils has been extensively evaluated through direct shear and root pull-out tests [1-6, among others], while the effects of: other stress paths that may lead to soil failure [7-9], hydraulic states and volumetric deformations upon shearing on soil reinforcement are still poorly investigated [10-14]. Given that vegetation strongly affects the soil-atmosphere interaction and that natural hazards are often triggered by phenomena that induce changes in soil water content [15-19], knowledge and laws from soil mechanics for partially saturated soils are essential to make considerations, tests and interpretation of the results.

Finally, in the framework of the geotechnical laboratory testing and especially for vegetated soils, the choice of a representative volume element has a prominent role on the significance and repeatability of tests. Morphological plant traits such the normalised volume of roots or root lengths with respect to soil volume should be assessed to both assess the representativeness of the in-situ conditions of the volume element and interpret the geotechnical results within a unified framework [20,21].

Considering all the above-mentioned, large cell triaxial compression tests will be carried out on fallow and vegetated samples at different degrees of saturation in this study. A protocol for soil compaction and root growth within soil samples will be defined and a shear strength criterion for partially saturated soils will be implemented with plant morpho-mechanical variables.

2 Material and experimental protocol

2.1 Soil used

Silty sand retrieved close the Llobregat river's delta in Barcelona was used. Its natural granulometric composition is: 41.2% of gravel, 28% of sand, 25.4% of silt and 5.4% of clay [14], it is a low-plasticity soil (plasticity index between 9.6 and 13.5%) with a density of solid particles is 2.65 Mg/m^3 [14]. The soil has been sieved through ASTM #4 (4.76 mm), to prepare the

* Corresponding author: alessandro.fraccica@isprambiente.it

testing samples. The bare and vegetated soil water retention curves were fitted using the model of [22], based on a modified form of the van Genuchten expression [23]:

$$S_r = C(s)(1/(1+(\alpha s)^n))^m \quad (1)$$

$$C(s)=1-(\ln(1+s/a)/\ln(2)) \quad (2)$$

Where s is matric suction, S_r the degree of saturation, $C(s)$ a function used to adjust the higher suction range of the curve. The air entry value is approximately linked to $1/\alpha$, the slope of the curve to n and the residual degree of saturation to m. The maximum suction corresponding to the residual degree of saturation is indicated by parameter a. The calibrated values of these parameters are provided in Table 1.

Table 1. Fitting parameters of the retention curves used in this study, from [14]

Soil	α (MPa^{-1})	n (-)	m (-)	a (MPa)
Bare	0.53	0.28	1.77	200
Vegetated	0.15	0.19	2.38	200

2.2 Sample compaction and test preparation

Soil samples were prepared by static compaction in PVC moulds, in eight layers each of 50 mm and diameter 200 mm. Scarifications were created with a spatula on the surface of each layer to ensure continuity with the upper layer. The total height of each sample was of 400 mm. Soil gravimetric water content and dry density at compaction were w = 15% and ρ_d = 1.6 Mg/m^3, respectively, as indicated by point A in Fig. ***1***, resulting in a degree of saturation S_r = 0.61, and a matric suction s = 40 kPa. The total vertical stress recorded on compaction was 100 kPa. The compaction state was chosen to be at dry of the optimum water content to create good physiological conditions for the plant to grow: a balanced proportion of air and water volumes in the voids and average macro-pore sizes consistent with root diameters. After compaction, the samples were seeded with *Cynodon dactylon* in 2-mm deep holes realized at a fixed spacing between each other (30 mm, Fig. ***1***) and at a given seeding density (i.e., 34 g/m^2). Finally, soil samples have been wetted to reach the hydraulic state indicated by point B in Fig. ***1*** (w = 21%, S_r = 0.84, matric suction s = 1 kPa) to induce plant growth, which lasted around eight months. Plant growth was deemed to be completed when observing roots at the bottom side of each specimen. A ceramic tip tensiometer (T5x UMS, München, Germany) allowed monitoring soil matric suction throughout the period of root development at 50 mm below the surface of the samples (Fig. ***1***).

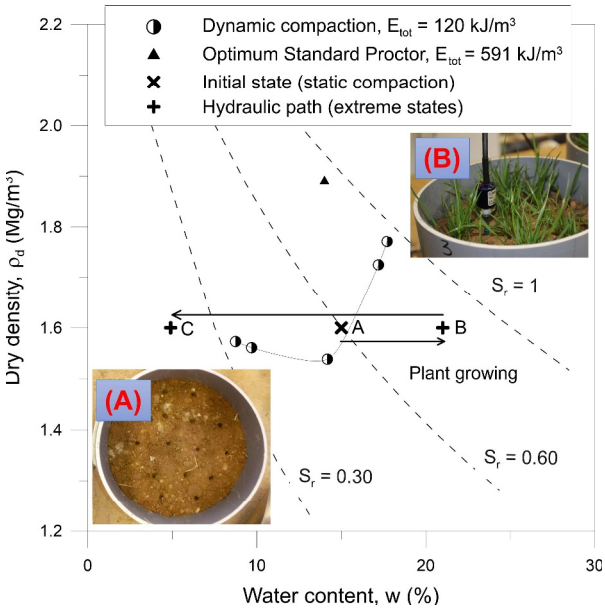

Fig. 1 Compaction plane and hydraulic states at compaction (A) and during root growth in samples (B)

Before being tested, soil samples were placed in a controlled-atmosphere room (T = 20±1°C and RH = 50±5%) to dry up the desired gravimetric content (evaluated by oven check [24], between points B and C in Fig. ***1***), then sealed in plastic sheet for 24 hours in darkness to equalise matric suction. At the end of this process, samples were extruded out of the PVC moulds by a piston moving at a constant rate (i.e., 1 mm/min) and pushed directly into the rubber membrane, whose internal surface was lubricated by oil to minimise the friction at the interface with soil. Matric and total suction, and the associated gravimetric water contents, were assessed before and after each test by a ceramic tip tensiometer, a chilled mirror dew point hygrometer (WP4, Decagon Devices, Pullman, WA, USA), and oven check, respectively, in four points of the samples. Two diametrically opposite measuring points were selected at the bottom and two at the upper surfaces of each sample, at 70 mm from its centre. Matric suction was not monitored continuously during the shearing phase.

2.3 Large cell triaxial equipment

The triaxial equipment used was developed in UPC geotechnical laboratory [25] to allow the testing of large samples (height = 400 mm and diameter = 200 mm). Confinement is applied by humid air (RH = 100%) pressure, checked by a pressure transducer, while axial and radial displacements in the samples are recorded by one vertical and twelve horizontal displacement transducers (LVDTs). Horizontal transducers are placed in contact with the sample's membrane through a system of regulating nuts, rods, o-rings and springs that crosses the steel cell at twelve positions, along two orthogonal directions and at three different heights of the sample (90-180-270 mm). See Fig. 2 and [25] for more details. Radial deformations were mathematically inferred as described in [14].

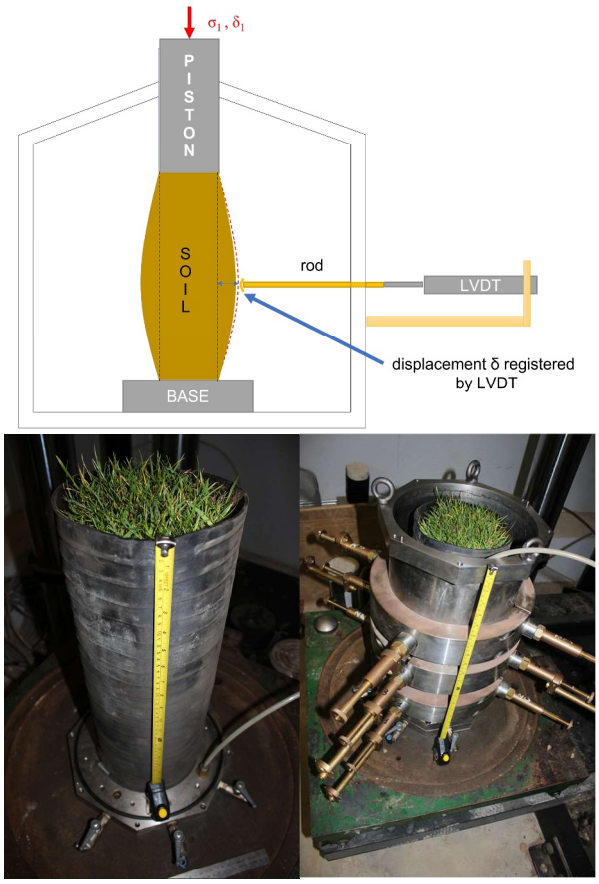

Fig. 2 Triaxial equipment with a vegetated sample and schematic operating principle of horizontal LVDTs of the equipment.

Tests were carried out on samples at constant water content conditions. Samples were firstly subjected to an isotropic compression, until a volumetric strain rate lower than 0.1%/day was observed. Then, triaxial drained compressions were carried out at a vertical displacement rate of 0.016 mm/min.

2.4 Roots volume and void ratio assessment

Void ratio was assessed at the end of each test by means of paraffin tests [26] on two points of each sample. Soil volumes inferred by paraffin method were corrected from the root volume contribution, according to the mathematical procedure described in [14]. Roots were retrieved after washing the soil samples and their volumes were inferred by image analysis and pycnometry. The root volume ratio, R_v (i.e., the normalised volume of roots by the unit volume of soil) observed in the tested samples ranged between 0.012 and 0.018.

3 Results

Fig. 3 presents an example of stress-strain (deviatoric stress q vs axial strain ε_{ax}) and volumetric strain (ε_{vol}) responses of vegetated and bare samples at low confinement and low matric suction. Root volume ratio R_v observed in the samples is indicated in the legend. Soil strength increase in vegetated soil was systematically observed after large deformations (i.e., around axial strain ε_{ax} = 4%) and without the possibility of reaching a stress plateau within the displacement range allowed by the equipment. Bare soil reached maximum strengths without observing a post-peak decrease. Volume deformations started to be higher in vegetated samples consistently with the trend described for the stress-strain curves.

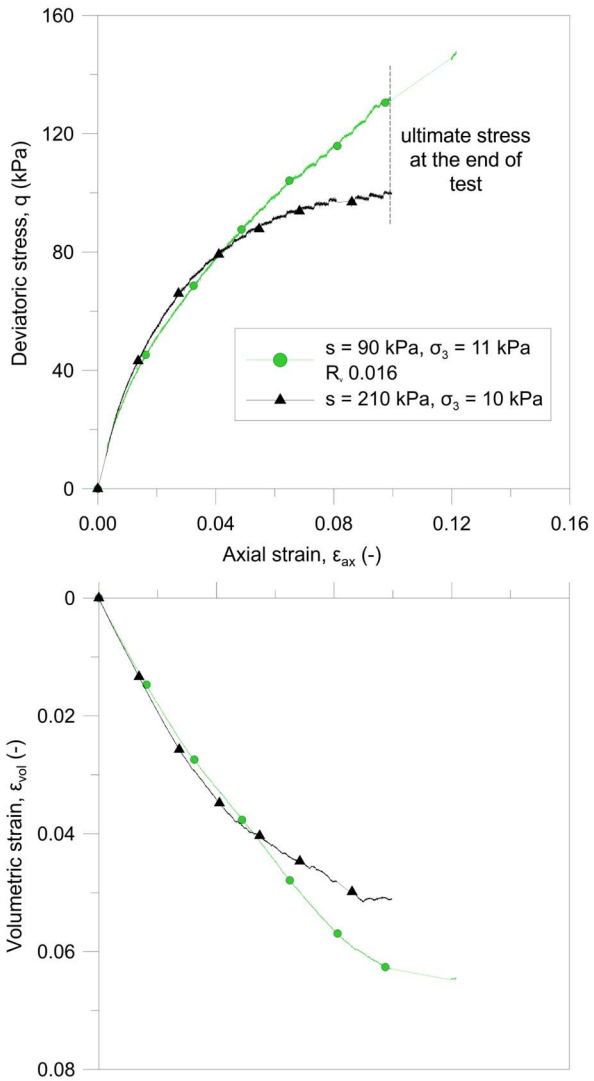

Fig. 3 Comparison of triaxial compression results on bare (black lines) and vegetated soil (green lines) at low matric suction.

An increase in strength and stiffness was generally observed in samples tested at drier hydraulic states. However, a different stress-strain response was observed in drier vegetated samples with respect to what was observed in Fig. 3. Indeed, drier vegetated samples exhibited more pronounced reinforcement and volume compression at small strains (i.e., around ε_{ax} = 1%), while almost reaching asymptotically the maximum stress level (Fig. 4). Void ratios at the end of the tests are reported in Table 2, jointly with the calculated average degree of saturation, the average of suction measurements and the root volume ratios. Despite higher void ratios were observed by [14] along drying trajectories on unconfined vegetated samples of the

same soil and roots, the void ratios observed after triaxial compressions were slightly smaller than those of bare samples at similar states and confinement, consistently with the higher volumetric deformations observed in the samples with roots. Root volume ratios were quite similar in all the vegetated samples, allowing a good confidence on the comparability of the results.

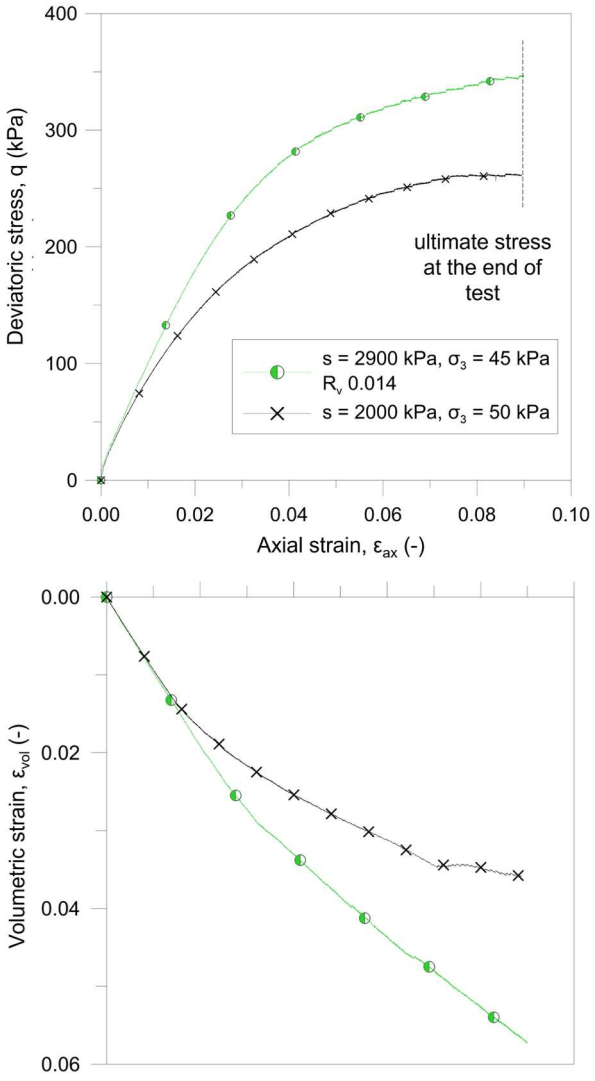

Fig. 4 Comparison of triaxial compression results on bare (black lines) and vegetated soil (green lines) at high matric suction.

4 Reinforcement interpretation

The failure criterion adopted to interpret the results was the Mohr-Coulomb for partially saturated soils based on the following constitutive stress formulation (σ', see e.g. [27-29]):

$$p' = p - u_a + S_{r,eff} s \; ; \; S_{r,eff} = S_r^{\alpha} \quad (3)$$

$$q = \sigma_1 - \sigma_3 \quad (4)$$

$$q_f = 6c' \cdot \cos\varphi' / (3 - \sin\varphi') + M_c \cdot p'_f \quad (5)$$

$$c' = c'_{bare} + c'_{roots} \; ; \; c'_{roots} = -\gamma \sigma_{tr} R_v \quad (6)$$

where p' and p'_f are the mean and ultimate mean skeleton stresses, p the total mean stress, u_a the air pressure, $S_{r,eff}$ is the effective degree of saturation (i.e. the degree of saturation in the soil macropores and evaluated as S_r elevated by α, the model parameter [29]). σ_1 and σ_3 are the vertical and confining total stresses, q is the deviator stress and the slope of the failure envelope is $Mc = 6 \sin\varphi'/(3-\sin\varphi')$, where φ' is the friction angle, and c' the cohesion. This last term was implemented with the root reinforcement term, modified from the formulation presented by [31], in which γ is the model parameter, σ_{tr} is the roots tensile strength (negative according to geotechnical conventional signs and whose value of – 2.35 MPa was measured through tensile tests on single roots by [14] for *Cynodon dactylon*), and R_v is the root volume ratio.

Table 2 Variables related to the hydraulic state and root volume ratios for vegetated (V) and bare (B) samples.

#	Final void ratio, e (-)	Average degree of saturation, Sr (-)	Average matric/total suction, s (kPa)	Confining total stress, σ_3 (kPa)	Root volume ratio, Rv (-)
B2	0.567	0.301	2000	50	-
B3	0.533	0.693	8	48	-
B4	0.589	0.527	95	40	-
B6	0.590	0.546	49	30	-
B8	0.571	0.619	38	50	-
B9	0.578	0.544	135	18	-
B10	0.606	0.593	50	21	-
B12	0.614	0.462	210	10	-
B13	0.600	0.457	250	30	-
B15	0.588	0.375	1780	25	-
V1	0.570	0.536	90	11	0.016
V2	0.658	0.242	3800	30	0.014
V3	0.657	0.213	4000	5	0.013
V4	0.512	0.779	12	10	0.014
V5	0.549	0.311	2900	45	0.014
V6	0.505	0.697	25	46	0.018
V7	0.481	0.938	1	30	0.012
V8	0.462	0.887	5	28	0.015

A calibration of two sets (for vegetated and bare soil) of α, M_C and γ using the Microsoft Excel's solver was carried out to minimise the squared error between q_f evaluated experimentally (as the ultimate stress at the end of test) and q_f formulated in the constitutive framework (equations 3 to 6). The values obtained are presented in Table 3.

Table 3 Calibrated parameters for the failure criterion framework used.

	Bare soil	Vegetated soil
α (-)	3.67	3.20
M_C (-)	1.42	1.45
γ (-)	-	0.30
c' (kPa)	0	10.3
φ' (°)	35.1	35.8

The two failure envelopes and the points at failure (p'_f, q_f) for each test, are plotted in Fig. 5. As it is possible to see, minor effects of vegetation on soil friction angle were observed, while roots contributed to increase the cohesion term. Friction values were in line with those observed in the same soil subjected to other stress paths [14, 30]. The calibrated γ parameter was far below the 1.2 evaluated by [31] and inferred from back-analysis on landslide vegetated scarps (where roots have been potentially subjected to larger deformations than in triaxial compressions). The α parameter is in line with those presented by [29] for similar kinds of soil. Vegetated soil presented a slightly lower α. This decrease is linked to the changes in the soil microstructure that roots generate during their growth: macropores enhancement due to fissuring and grain displacements and partial clogging of micro-pores due to complex chemo-mechanical interactions. This change in soil structure is affecting the water retention properties and the volume change behaviour observed upon shearing.

Although the failure stress states of vegetated soil were successfully represented by a failure criterion, the stress-strain responses of soil with roots were strongly affected by the hydraulic states (Fig. 3 and Fig. 4): at low values of suction, the small confinement at the soil-root interaction made the roots stretch and align before generating some reinforcement in the soil due to the friction generated by fibres pull-out. Similar trends were observed in plant- and fibre-reinforced soils [5, 32-34]. On the contrary, shrinkage upon drying and higher suction values contributed to increase soil confinement around roots, and in turn impeded differential displacements at the soil-root interface. Hence the elastic properties and the tensile strength of roots were better exploited in reinforcing the soil.

Fig. 6 reports the secant Young Modulus values calculated along the triaxial compression stress-strain curves, at axial strain ε_{ax} = 1% as function of the confining skeleton stress σ'_3. Vegetation roots slightly contributed to increase soil stiffness too. This observation could be in part explained because *Cynodon dactylon* has roots spreading in all the directions within the samples [14]: tensile forces developed within those inclined towards the outer lateral surface, due to soil radial strains. In turn these forces had a component in the radial direction of the samples, generating an additional confining effect which made the vegetated soil response stiffer.

5 Conclusions

This study presented laboratory results and vegetation reinforcement interpretation on a partially saturated silty sand tested under triaxial compression in a large cell equipment.

A unique protocol was followed for the preparation of all the samples: soil was compacted at the same hydraulic state and dry density, then wetted under unconfined conditions to let the plants grow and finally dried to the desired matric suctions. Bare soil underwent the same hydro-mechanical history for the sake of comparison.

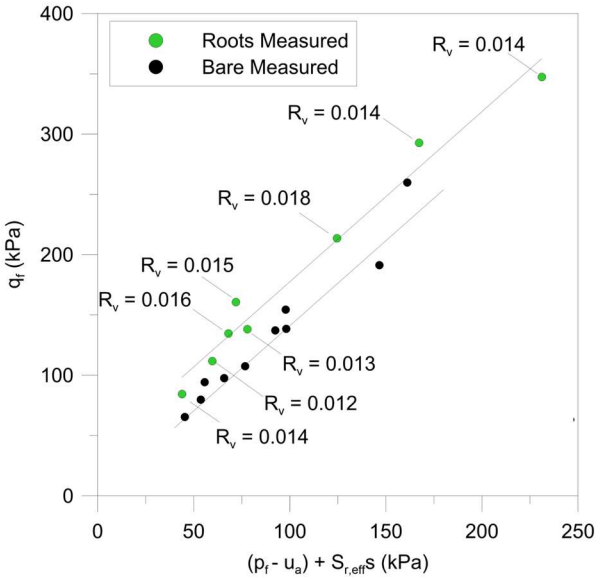

Fig. 5 Failure envelopes and q_f / p'_f end-of-test states for bare and vegetated soil

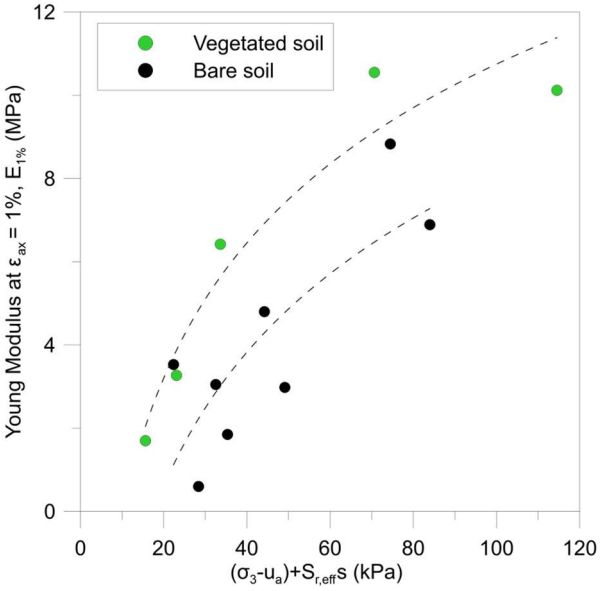

Fig. 6 Comparison of Young Modulus values calculated on stress-strain triaxial test curves, at 1% of axial deformation.

Tests on vegetated soils were carried out after 8 months of plant growing periods. After each test, the normalised volume of roots by the unit volume of soil was assessed. Roots affected soil mechanical response in different ways depending on the suction level: close to saturation roots more likely were stretched and pulled out, generating friction forces at the soil interface, and inducing a constant increase in soil shear stresses. When soil was drier, the higher embedment of roots caused by soil shrinkage and higher suction at the soil-roots interface impeded large roots displacements within the matrix, hence exploiting their tensile strength and generating a root reinforcement mechanism typical of fibre breakage.

Soil matric/total suction was measured before and after the tests while the degree of saturation evaluated through water content and void ratio checks at the end of each test.

The results were successfully interpreted within a failure criterion and skeleton stress framework for partially saturated soils, considering soil suction, degree of saturation, and soil microstructure. The good result in representing vegetated samples at different confinements by a unique failure criterion is indicative that a good repeatability was ensured by the large size of the samples, given that they had very similar root volumes ratios. Hence the failure criterion was implemented to predict the effect of this morphological trait of roots and their tensile strength on soil shear strength increase.

As vegetated and fallow soil failure envelopes were traced considering the ultimate strength recorded in each test, it was observed that they differed essentially in the cohesion term. However, this shear strength parameter has been found to be strongly linked to soil shear deformation and in turn to the stretching of root fibres.

The authors wish to acknowledge the support of the European Commission via the Marie Skłodowska-Curie Innovative Training Networks (ITN-ETN) project TERRE 'Training Engineers and Researchers to Rethink geotechnical Engineering for a low carbon future' (H2020-MSCA-ITN-2015-675762).

References

1. A. Yildiz, F. Graf, C. Rickli, S.M. Springman, Catena, **166**, 98–113 (2018)
2. A. Gonzalez-Ollauri, S. Mickovski, Geoderma, **285**, 141–150 (2017)
3. C. Fan, C. Su. Ecol. Eng, **33**(2), 157–166 (2008)
4. E. Comino, P. Marengo, V. Rolli, Soil Tillage Res. **110**(1), 60–68 (2010)
5. N. Pollen, N., Catena **69**, 197–205 (2007)
6. S.B. Mickovski, A.G. Bengough, M.F. Bransby, M.C.R. Davies, P.D. Hallett, and R. Sonnenberg, Eur. J. Soil Sci. **58**, 1471–1481 (2007)
7. G. Chen, S. Zheng, J. Zhu, W. Wang, W. Feng, Landslides, **17**, 471–482 (2020)
8. D.M. Potts, L. Zdravkovic *Finite Element Analysis in Geotechnical Engineering: Theory*' Thomas Telford Publishing. 1 Heron Quay, London: Thomas Telford Ltd, EI44JD (1999)
9. Y.J. Cui, P. Delage Géotechnique. **46**(2), 291–311 (1996)
10. C.B. Zhang, L.H. Chen, Y.P. Liu, X.D. Ji, X.P. Liu, Ecol. Eng., **36**(1), 19–26, (2010)
11. Y. Li, Y. Wang, Y. Wang, C. Ma, Sci Rep., **7**,800 (2017)
12. X. Ji, IOP Conf Ser Earth Environ Sci., **304**, 032106 (2019)
13. A.A. Karimzadeh, A.K. Leung, S. Hosseinpour, Z. Wu, P.F. Amini, Can Geotech J, **58**(12), 1915-1927 (2021)
14. A. Fraccica *Experimental Study and Numerical Modelling of Soil-Roots Hydro-Mechanical Interactions.* (PhD Thesis) Universitat Politècnica de Catalunya (Spain), Université de Montpellier (France) (2019)
15. E.E. Alonso, A. Gens, C.H. Delahaye, Hydrogeol J. **11**, 174–192 (2003)
16. G. Yanamandra, W.T. Oh, Int. J. Geomech., **21**(10), 04021199 (2021)
17. P.J. Vardon, Environ. Geotech., **2**, 166–174 (2015)
18. A. Yildiz, F. Graf, and S.M. Springman, Proc. Inst. Civ. Eng.: Geotech. **172**(6), 520-529 (2019)
19. K. Mahannopkul and A. Jotisankasa, Soils Found, **59**(2), 500-516 (2019)
20. T.H. Wu, W.P. McKinnell III, D.N. Swanston, Can Geotech J., **16**(1), 19–33 (1979)
21. M. Schwarz, P. Lehmann, D. Or, Earth Surf Process Landf., **35**, 354–367 (2010)
22. E. Romero and J. Vaunat. *Retention curves of deformable clays*, in Proceedings of the International Workshop on Unsaturated Soils: Experimental Evidence and Theoretical Approaches in Unsaturated Soils, 91–106 (2000)
23. M.T. van Genuchten. Soil Sci. Soc. Am. J., **44**, 892–898 (1980)
24. ASTM D2216 *Standard Test Methods for Laboratory Determination of Water (Moisture) Content of Soil and Rock by Mass* www.astm.org (2019)
25. C.E. Alvarado de Menéndez, *Comportamiento hidro-mecánico de agregados gruesos*. (PhD Thesis), Universitat Politècnica de Catalunya (Spain) (2017)
26. ASTM D7263 *Standard Test Method fo Laboratory Determination of Density (Unit Weigth) of Soil Specimens.* www.astm.org (2018)
27. S.K. Vanapalli, D.G. Fredlund, D.E. Pufahl, and A.W. Clifton. Can. Geotech. J., **33**(3), 379-392 (1996)
28. A. Tarantino, S. Tombolato, Géotechnique, **55**(4), 307–317 (2005)
29. E.E. Alonso, J.M. Pereira, J. Vaunat, S. Olivella S., Géotechnique, **60**(12), 913–925 (2010)
30. A. Fraccica, E. Romero, and T. Fourcaud, Geomech. Energy Environ., 30, 100303 (2022)
31. T.H. Wu, W.P. McKinnell III, and D.N. Swanston, Can. Geotech. J., **16**, 19–33 (1979)
32. A. Diambra, E. Ibraim, D. Wood Muir, A.R. Russell, Geotext Geomembr, **28**(3), 238–250 (2010)
33. C. Tang C, B. Shi, W. Gao, F. Chen, Y. Cai Geotext Geomembr. **25**(3), 194–202 (2007)
34. K.S. Heineck, M.R. Coop, N.C. Consoli, J Geotech Geoenviron. Eng. **131**(8), 1024–1033 (2005)